

■ Natural Products

Hybridorubrins A–D: Azaphilone Heterodimers from Stromata of *Hypoxylon fragiforme* and Insights into the Biosynthetic Machinery for Azaphilone Diversification

Kevin Becker,^[a, b] Sebastian Pfütze,^[a, b] Eric Kuhnert,^[c, d] Russell J. Cox,^[c, d] Marc Stadler,^{*[a, b]} and Frank Surup^{*[a, b]}

Abstract: The diversity of azaphilones in stromatal extracts of the fungus *Hypoxylon fragiforme* was investigated and linked to their biosynthetic machineries by using bioinformatics. Nineteen azaphilone-type compounds were isolated and characterized by NMR spectroscopy and mass spectrometry, and their absolute stereoconfigurations were assigned by using Mosher ester analysis and electronic circular dichroism spectroscopy. Four unprecedented bis-azaphilones, named hybridorubrins A–D, were elucidated, in addition to new fragirubrins F and G and various known mitorubrin derivatives. Only the hybridorubrins, which are composed of mitorubrin and fragirubrin moieties, exhibited strong inhibi-

tion of *Staphylococcus aureus* biofilm formation. Analysis of the genome of *H. fragiforme* revealed the presence of two separate biosynthetic gene clusters (BGCs) *hfaza1* and *hfaza2* responsible for azaphilone formation. While the *hfaza1* BGC likely encodes the assembly of the backbone and addition of fatty acid moieties to yield the (*R*)-configured series of fragirubrins, the *hfaza2* BGC contains the necessary genes to synthesise the widely distributed (*S*)-mitorubrins. This study is the first example of two distant cross-acting fungal BGCs collaborating to produce two families of azaphilones and bis-azaphilones derived therefrom.

Introduction

The Hypoxylaceae, which were recently resurrected in the course of a major phylogenetic study, are the second largest family of the ascomycete order Xylariales,^[1] and they are known for a particularly diverse secondary metabolism.^[2] In contrast to other families of the order, both their mycelial cul-


tures and their stromata (a mass of fungal tissue that has embedded spore-bearing structures such as ascomata) have been shown to contain diverse pigments and other secondary metabolites. The first of these pigments were reported in 1974 by Steglich et al. from *Hypoxylon fragiforme*, the type species of the largest genus of the Hypoxylaceae, and shown to belong to the mitorubrin-azaphilone class of metabolites.^[3] Several years later, the same species was subjected to an intensive study, and various cytochalasans and other unknown compounds were detected and isolated from the young, growing stromata.^[4] In the same study, it was found that the composition of secondary metabolite profiles differs drastically during the vegetative growth period, and this points toward differential activation of secondary metabolite biosynthesis genes. From cultures of the fungus, several different metabolites such as dihydroisocoumarins,^[5] a dibenzoxanthenone,^[6] various cytochalasans,^[7] and small polyketides have been reported.^[8] Some of these metabolites were found to have prominent activities in biological systems, while others, like the complex azaphilones that were recently detected in fossil stromata of *H. fragiforme* and isolated from freshly collected material, are unprecedented compounds.^[1b] We have recently started to further evaluate the diversity of secondary metabolites in twelve selected species of the Hypoxylaceae for which we generated high-quality genome sequences with the aim of establishing correlations between the biological and chemical diversity in these organisms at the genomic level.^[9] The ex-epitype strain of *H. fragiforme*, the type species of the genus *Hypoxylon* and


[a] K. Becker, S. Pfütze, Prof. Dr. M. Stadler, Dr. F. Surup
Department Microbial Drugs
Helmholtz Centre for Infection Research GmbH (HZI)
Inhoffenstrasse 7, 38124 Braunschweig (Germany)
E-mail: marc.stadler@helmholtz-hzi.de
frank.surup@helmholtz-hzi.de

[b] K. Becker, S. Pfütze, Prof. Dr. M. Stadler, Dr. F. Surup
German Centre for Infection Research Association (DZIF)
Partner site Hannover-Braunschweig, Inhoffenstrasse 7
38124 Braunschweig (Germany)

[c] Dr. E. Kuhnert, Prof. Dr. R. J. Cox
Institute for Organic Chemistry, Leibniz University Hannover
Schneiderberg 1B, 30167 Hannover (Germany)

[d] Dr. E. Kuhnert, Prof. Dr. R. J. Cox
Centre for Biomolecular Drug Research (BMWZ)
Schneiderberg 38, 30167 Hannover (Germany)

 Supporting information and the ORCID identification number(s) for the author(s) of this article can be found under:
<https://doi.org/10.1002/chem.202003215>.

 © 2020 The Authors. Chemistry - A European Journal published by Wiley-VCH GmbH. This is an open access article under the terms of the Creative Commons Attribution License, which permits use, distribution and reproduction in any medium, provided the original work is properly cited.

the most frequently encountered species in the Northern hemisphere, was selected for genome sequencing. As expected from the various reports on the chemical diversity of secondary metabolites, the genome harbours a great many biosynthetic gene clusters (BGCs) that putatively encode the biosynthesis of various polyketide and polyketide–peptide hybrids. We have recently reported on the identity of the cytochalasin gene cluster of this fungus and its partial heterologous expression in *Magnaporthe grisea*.^[10] Furthermore, we reported the occurrence of the novel azaphilones fragirubins A–E and the bis-azaphilones rutilins C and D in stromata of *H. fragiforme* in addition to the known mitorubins.^[1b] The present study deals with the isolation and identification of azaphilone heterodimers with interesting structural and biological features, as well as the assignment of their biosynthesis genes.

Results and Discussion

Isolation and structure elucidation

Freshly collected stromata of *Hypoxylon fragiforme* were extracted with acetone. In the crude extract the new compounds 1–6 (Figure 1) were detected by HR-ESI-MS analysis and subsequently purified by preparative chromatography. Proton and carbon NMR data of the pure 1–6 are given in Tables 1 and 2.

Hybridorubrin A (1) was shown to have the molecular formula $C_{52}H_{62}O_{15}$ by HR-ESI-MS. The IR spectrum of 1 showed characteristic absorptions at $\tilde{\nu}_{\max} = 1717$ and 1621 cm^{-1} , representing ester and conjugated double bonds, respectively (Figure S42 in the Supporting Information). In the ^1H and $^1\text{H}/^{13}\text{C}$ HSQC NMR spectra, the presence of six methyl groups, two methylene groups, and an uncertain number of methylene groups in an alkyl chain, as well as one two aliphatic and nine aromatic/olefinic methine groups, was observed. The ^{13}C and $^1\text{H}/^{13}\text{C}$ HMBC spectra showed the presence of four conjugated keto groups, three carboxylic ester groups, as well as eleven sp^2 - and two sp^3 -hybridized carbon atoms.

$^1\text{H}/^1\text{H}$ COSY signals (Figure 2) revealed 12- H_2 , 13-H, and 14- H_3 to be contiguous. For the propyl chain protons 12a- H_2 , 13a-H, and 14a- H_3 , a similar link was established. The first azaphilone core was identified by $^1\text{H}/^{13}\text{C}$ HMBC correlations (Figure 2) from 4-H to C-3, C-6, and C-10, from 1- H_2 to C-3, C-5, C-9, and C-10, as well as from 11- H_3 to C-7, C-8, and C-9. Mutual correlations of 4-H and 12- H_2 linked C-12 to C-3. An acetate moiety was connected to C-13 by correlations from 13-H to C-15 and from 16- H_3 to C-12. The second azaphilone unit was established analogously. Correlations from 13_a-H to C-6 as well as 14a-H to C-5, C-6, and C-7 linked the two azaphilone units. The *Z* configuration of the $\Delta^{6,14a}$ alkene was deduced from the presence of a strong $^1\text{H}/^1\text{H}$ ROESY correlation between 14a-H and 4-H (Figure 2 and Figure S10 in the Supporting Information), while that of the $\Delta^{12a,13a}$ alkene was determined as *E* from the coupling constant of the respective protons ($^3J = 15.3\text{ Hz}$).

For the fatty acid moiety, the carboxylic terminus was established by $^1\text{H}/^1\text{H}$ COSY correlations linking 2'- H_2 , 3'- H_2 , and 4'- H_2 as well as by $^1\text{H}/^{13}\text{C}$ HMBC correlations from 3'- H_2 to C-1', C-2',

C-4', and C-5'. The methyl terminus 16'- H_3 showed correlations to C-15' and C-14', which were supported by $^1\text{H}/^1\text{H}$ COSY data. The hydroxyl group 13'-OH showed $^1\text{H}/^{13}\text{C}$ HMBC correlations to C-12', C-13', and C-14'. The methylene 12'- H_2 had a correlation to C-11', which was accordingly placed in the alkyl chain. The missing signals for C-5' to C-10' overlap and could not be assigned unambiguously. Consequently, the length of the fatty acid chain was deduced from the molecular formula of 1. By using Mosher's method,^[11] the stereochemistry of C-13' was assigned as (*R*) (Figure S38 in the Supporting Information). Ultimately, the fatty acid moiety of 1 was deduced to be (*R*)-13'-hydroxypalmitic acid. The fatty acid was linked to C-8 by $^4J\ ^1\text{H}/^{13}\text{C}$ HMBC correlations from 11- H_3 to C'-1 and from 2'- H_2 to C-8. Lastly, the orsellinic acid moiety was established by $^1\text{H}/^{13}\text{C}$ HMBC correlations of 7a'- H_3 to C-1a', C-5a', C-6a', and C-8a', from 4a'-OH to C-3a', C-4a', and C-5a', as well as from 2a'-OH to C-1a', C-2a', and C-3a'. Correlations from 11a- H_3 to C-8a' linked the orsellinic acid to C-8a. The stereochemistry of C-8(*R*) and C-8a(*S*) was deduced from their respective building blocks mitorubrin and fragirubrin (see Stereochemistry section below for details). Due to occurrence of a fragirubrin building block in 1, the stereochemistry of C-13(*S*) was deduced from the fragirubins.^[1b] Eventually, the same C-13(*S*) configuration was also found in lenormandin F.^[12]

Analysis of hybridorubrin B (2) revealed its molecular formula to be $C_{54}H_{62}O_{15}$, indicating two additional carbon atoms and two additional degrees of unsaturation compared with 1. Instead of (*R*)-13'-hydroxypalmitic acid, it bears (*R*)-16'-hydroxylinoleic acid, as shown by its NMR data. The stereochemistry of C-16' was assigned by Mosher's method (Figure S39 in the Supporting Information). The chemical shifts of C-8' and C-14' were characteristic for a *cis* (*Z*)/*cis* (*Z*) 1,4-diene configuration of $\Delta^{9,10'}$ and $\Delta^{12',13'}$.^[13]

Hybridorubrin C (3) has a molecular formula of $C_{54}H_{64}O_{15}$, as shown by HR-ESI-MS data. This implied a formal loss of hydrogen relative to 1, representing one additional degree of unsaturation, while having a fatty acid moiety extended by two carbon atoms. Accordingly, two olefinic protons were observed in the $^1\text{H}/^{13}\text{C}$ HSQC spectrum and placed in the fatty acid chain of 3. The exact position of the alkene was deduced to be $\Delta^{9,10'}$ due to occurrence of two diagnostic MS/MS fragments (*m/z* 155.1123 and 171.1066) after epoxidation of the double bond (see Experimental Section and Figure S45 in the Supporting Information).^[14] The stereochemistry of this alkene was determined as *cis* (*Z*) from comparison of chemical shifts of the allylic carbon atoms C-8' and C-11' (both $\delta_{\text{C}} = 27.4$).^[15] By applying Mosher's method, the stereochemistry of C-17'(*R*) was deduced (Figure S40 in the Supporting Information).

Hybridorubrin D (4) showed a molecular formula of $C_{50}H_{60}O_{13}$, implying the formal loss of a $\text{C}_2\text{H}_2\text{O}_2$ fragment compared to 1. The NMR spectra of 4 were highly similar to those of 1, with the key differences being the lack of an acetyl group attached to O-13 as well as a different fatty acid moiety, which was identified as palmitic acid.

The molecular formula of fragirubrin F (5) was determined from its HR-ESI-MS data as $C_{31}H_{46}O_8$. Its ^1H and ^{13}C NMR data showed high similarity to those of fragirubrin A (15).^[1b] Com-

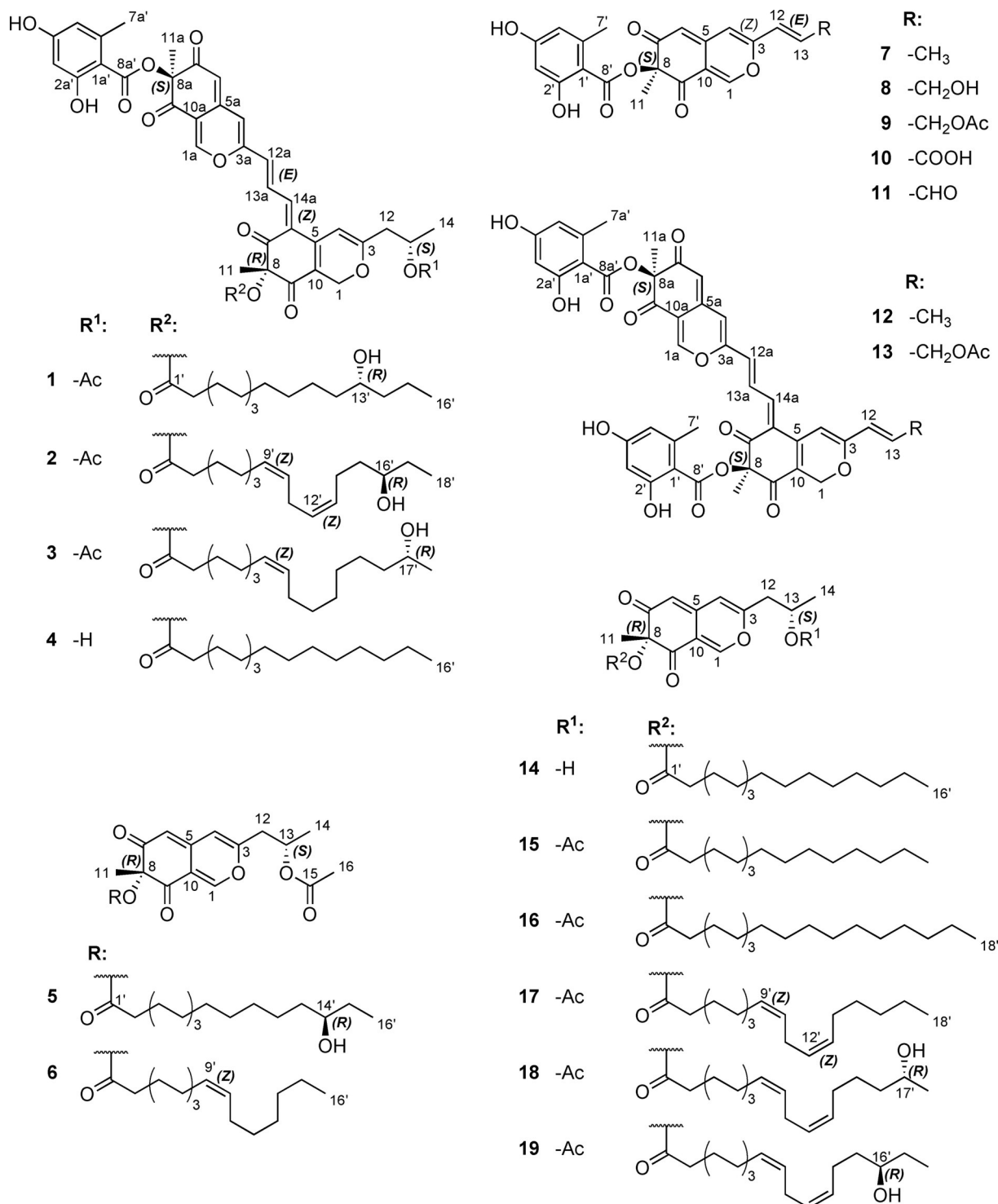


Figure 1. Structures of new (left) and known (right) azaphilones isolated from the stomata of *Hypoxyylon fragiforme*: **1–4**: hybridorubins A–D; **5–6**: fragirubins F–G; **7**: mitorubrin; **8**: mitorubrinol; **9**: mitorubrinol acetate; **10**: mitorubrinic acid; **11**: mitorubrinol; **12–13**: rutilins C–D; **14**: lenormandin F; **15–19**: fragirubins A–E.

pound **5** contains four methyl groups, three olefinic and two aliphatic methine groups, as well as 14 methylene groups. Additionally, signals for two conjugated keto groups, two ester carbonyl groups, one oxygenated sp³ carbon atom and three sp² carbon atoms were observed in the ¹³C NMR spectra. The main difference to **15** was the replacement of the palmitoyl

moiety by (*R*)-14'-hydroxypalmitic acid. The absolute stereochemistry of C-14' was determined by using Mosher's method (Figure S41 in the Supporting Information).

HR-ESI-MS data determined the molecular formula of fragirubrin G (**6**) as C₃₁H₄₄O₇, implying one additional degree of unsaturation relative to fragirubrin A (**15**). The ¹H and ¹H/¹³C HSQC

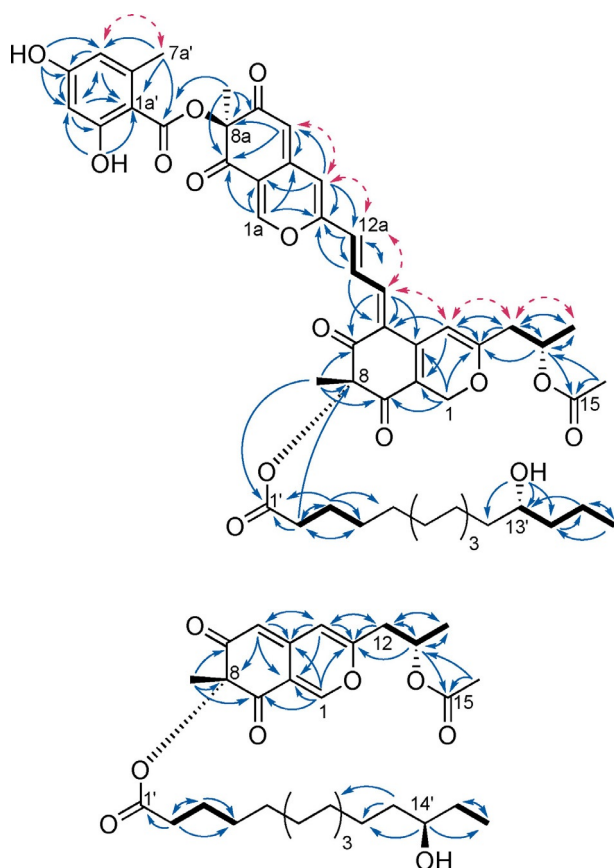


Figure 2. Key NMR correlations of hybridorubrin A (1) and fragirubrin F (5). Bold bonds: $^1\text{H}/^1\text{H}$ COSY correlations; solid, blue arrows: $^1\text{H}/^{13}\text{C}$ HMBC correlations; dashed, pink arrows: $^1\text{H}/^1\text{H}$ ROESY correlations.

spectra located an additional olefin in the fatty acid moiety ($\Delta^{9,10}$). The position and stereochemistry of this double bond was determined by degradation of the compound to its fatty acid methyl ester (**6-FAME**) and subsequent comparison of GC retention times with those of authentic standards, which resulted in the identification of 9-*cis* (*Z*)-hexadecenoic acid (palmitoleic acid; see Figure S46 in the Supporting Information and Experimental Section).

Stereochemistry of azaphilones occurring in *H. fragiforme* and revision of rutilins C and D

The stereochemistry of the azaphilones, particularly of C-8 in the backbone, is an important aspect of structural complexity. While the first occurrence of (–)-mitorubrins was described in 1965 by Büchi et al. from cultures of *Penicillium rubrum*^[16] (current name: *Talaromyces ruber*), Steglich et al. later described (+)-stereoisomers of mitorubrins from the stromata of *H. fragiforme*.^[3] Curiously, the genus *Talaromyces* was reported to contain either (+)- or (–)-mitorubrins depending on the species.^[17]

We utilized electronic circular dichroism (ECD) spectroscopy as a means to assess the stereochemistry of the monomeric azaphilones. A study by Clark et al. on chemical synthesis of the azaphilone backbone^[18] allowed for relatively simple assignment: mitorubrinol (**8**) from *H. fragiforme* showed a posi-

tive cotton effect (CE) at 245 nm and negative CE at 226 and 272 nm (Figure S44 in the Supporting Information). These ECD data indicate an (*S*)-(+)-configuration,^[18] which we conferred to all mitorubrin-type azaphilones from *H. fragiforme* due to their common biosynthetic origin (see Biosynthesis section for details). However, all fragirubrins^[1b] showed inverted ECD spectra with positive CE at about 230 and 274 nm and negative CE around 250 nm, accordingly rendering them (*R*)-(–) isomers (Figure S44 in the Supporting Information).

Taking the ECD results and the BGC analysis (see Biosynthesis section below) into account then allows for stereochemical assignment of the heterodimers: rutilins such as **12–13**, which consist of two (*S*)-mitorubrin-type building blocks, are hence (*S*)-configured at both C-8 and C-8a. Hybridorubrins **1–4**, in turn, are (*S*)-configured at C-8a in their mitorubrin moiety and (*R*)-configured at C-8 in their fragirubrin part. We hence have to revise data from our prior study with rutilins C (**12**) and D (**13**), and the mitorubrins,^[1b] to be (*S*)-configured at C-8 and C-8a.

Bioactivity testing

Compounds **1–2**, **4–10**, and **12–18** were tested for their antimicrobial activity in a minimum inhibitory concentration (MIC) assay as well as for their cytotoxicity, but were found to be devoid of activity against the examined test organisms or cell lines (Table S3 in the Supporting Information). The lack of antimicrobial and cytotoxic activities is largely in accordance with former findings for mitorubrin-type azaphilones.^[4]

In addition, **1**, **3–4**, **7–10**, **12**, and **14–15** were tested for their inhibitory effect on biofilm formation of *Staphylococcus aureus* (Table 3). Due to minor impurities in the samples, the given percentage values only allow for a rough estimation of bioactivity. Strong activity was observed for the bis-azaphilones hybridorubrins A (**1**), C (**3**), D (**4**), and rutilin C (**12**). These compounds have potency similar to that of the reference microporenic acid A,^[19] as well as sclerin, and sclerin diacid from *H. fragiforme*.^[8] The mitorubrin-type azaphilones **7** and **9**, as well as the fatty acid-containing **15**, showed weak activity, while **8**, **10**, and **14** showed no inhibition.

These results allow for preliminary structure–activity relationships to be deduced: since rutilin C (**12**) showed much stronger inhibition of biofilm formation than **7**, a strong influence of the fused second azaphilone backbone is suggested. In addition, the differing inhibition of biofilm formation of the mitorubrin-type azaphilones **7–10** indicates a modest influence of the functional group at C-14: a methyl group or an acetate unit (**7**, **9**) allowed for weak activity, while azaphilones carrying more polar hydroxyl or carboxylic acid moieties at C-14 (**8**, **10**) exhibited no inhibition of biofilm formation.

Lenormandin F (**14**) and fragirubrin A (**15**), which both carry a C_{16} fatty acid moiety instead of an orsellinic acid residue at C-8, only differ in the presence of an acetate moiety at C-13 in **15**. While **14** showed no activity, **15** exhibited weak activity similar to **7** and **9**. Hence, a positive effect of C-13 acetylation can be deduced. By comparing **7** and **9** to **15**, the presence of an orsellinic acid or a fatty acid moiety at C-8 does not seem

Table 1. ¹H NMR spectroscopic data [ppm] of hybridorubrins A–D (1–4) and fragirubrins F–G (5–6) (1, 3–4, 6: 700 MHz; 2, 5: 500 MHz).

Position	1 ^[a]	2 ^[b]	3 ^[a]	4 ^[a]	5 ^[a]	6 ^[b]
1	5.07, d (13.6); 4.84, d (13.6)	5.18, d (14.0); 4.87, d (14.0)	5.07, d (13.6); 4.84, d (13.6)	5.02, d (13.6); 4.94, d (13.6)	8.00, d (1.1)	7.85, s
4	6.13, s	5.71, s	6.13, s	6.09, s	6.45, s	6.14, s
6	–	–	–	–	5.47, d (1.1)	5.54, s
11	1.53, s	1.57, s	1.53, s	1.53, m	1.45, s	1.54, s
12	2.63, dd (14.4, 7.7); 2.57, dd (14.4, 5.2)	2.61, dd (14.6, 8.0); 2.49, dd (14.6, 5.0)	2.61, dd (14.3, 8.0); 2.57, dd (14.3, 5.4)	2.46, dd (14.2, 7.7); 2.41, dd (14.2, 5.2)	2.76, d (6.4)	2.69, dd (14.7, 7.3); 2.61, dd (14.7, 5.3)
13	5.19, dqd; (7.7, 6.5, 5.2)	5.25, m	5.19, m	4.10, m	5.17, tq (2×6.4)	5.17, m
14	1.30, d (6.5)	1.34, d (6.2)	1.30, d (6.2)	1.22, d (6.2)	1.31, d (6.3)	1.33, d (6.5)
16	1.99, s	2.07, s	1.99, s	–	1.98, s	2.06, s
2'	2.41, t (7.3)	2.46, t (7.7)	2.42, t (7.4)	2.41, t (7.5)	2.36, t (7.4)	2.45, t (7.4)
3'	1.62, m	1.66, m	1.62, td (7.4, 1.8)	1.61, m	1.59, tt (2×7.4)	1.63, m
4'	1.39, m	1.36, m	1.40, m	1.40, m	1.37, m	1.35, m
5'–7'	1.31, m ^[c]	1.32, m ^[c]	1.35, m ^[c]	1.29, m ^[c]	1.30, m ^[c]	1.30, m ^[c]
8'	1.31, m ^[c]	2.05, m	2.05, m ^[c]	1.29, m ^[c]	1.30, m ^[c]	2.01, m ^[c]
9'	1.31, m ^[c]	5.39, m	5.35, m ^[c]	1.29, m ^[c]	1.30, m ^[c]	5.35, m ^[c]
10'	1.31, m ^[c]	5.34, m	5.35, m ^[c]	1.29, m ^[c]	1.30, m ^[c]	5.35, m ^[c]
11'	1.45/1.32, m	2.80, dd (2×6.7)	2.05, m ^[c]	1.29, m ^[c]	1.30, m ^[c]	2.01, m ^[c]
12'	1.39, m	5.38, m	1.35, m ^[c]	1.29, m ^[c]	1.44, m; 1.33, m	1.30, m ^[c]
13'	3.50, m	5.39, dd (9.3, 4.3)	1.35, m ^[c]	1.29, m ^[c]	1.37, m	1.30, m ^[c]
14'	1.36, m	2.18, m; 2.16, m	1.35, m ^[c]	1.27, m	3.42, brs	1.27, m
15'	1.36, m	1.51, m	1.31, m	1.29, m	1.44, m; 1.37, m	1.30, m
16'	0.88, t (7.1)	3.56, m	1.38, m	0.88, t (7.1)	0.90, t (7.3)	0.89, d (6.7)
17'	–	1.49, m	3.69, dt; (10.5, 5.9)	–	–	–
18'	–	0.95, t (7.4)	1.10, d (5.9)	–	–	–
1a	8.21, s	7.98, s	8.21, d (0.9)	8.21, d (1.1)	–	–
4a	6.89, s	6.45, s	6.89, s	6.88, s	–	–
6a	5.74, d (0.9)	5.76, s	5.74, d (0.9)	5.74, d (1.1)	–	–
11a	1.68, s	1.69, s	1.68, s	1.68, m	–	–
12a	7.02, d (15.3)	6.59, d (15.3)	7.01, d (15.2)	7.04, d (15.1)	–	–
13a	8.05, dd (15.3, 11.8)	8.01, dd (15.3, 11.7)	8.05, dd (15.2, 11.6)	8.05, dd (15.1, 11.8)	–	–
14a	7.54, d (11.8)	7.02, d (11.7)	7.54, br d (11.6)	7.56, d (11.8)	–	–
3a'	6.24, d (2.4)	6.18, d (2.2)	6.23, d (2.4)	6.23, d (2.4)	–	–
5a'	6.36, m	6.21, d (2.2)	6.36, d (2.4)	6.36, m	–	–
7a'	2.61, m	2.61, m	2.61, s	2.61, s	–	–
2a'-OH	10.74, s	10.75, s	10.74, s	10.74, s	–	–
4a'-OH	9.24, s	n/a ^[d]	9.26, s	9.24, s	–	–
misc.	13'-OH; 3.22, d (5.4)	16'-OH; n/a ^[d]	17'-OH; 3.31, d (4.7)	13-OH; 3.92, d (4.7)	14'-OH; n/a ^[d]	–

[a] [D₆]acetone. [b] CDCl₃. [c] Signals could not be unambiguously assigned due to overlaps. [d] No signals observed.

to be highly relevant for activity against *S. aureus* biofilm formation.

Taking these findings into account, the strong bioactivity measured for hybridorubrins A (1), C (3), and D (4) and rutilin C (12) can be mainly explained by the fusion of two azaphilone building blocks. As acetylation of C-13 was deduced to be beneficial for bioactivity, 4 consequently exhibited a weaker effect than 1 and 3.

Azaphilone BGC analysis

In order to understand how the wide diversity of azaphilone-type compounds in the stromata of *H. fragiforme* is genetically encoded, we investigated the genome sequence of the producer organism. Genome sequencing of the fungus had been performed in the context of a previous study.^[9]

To identify a likely candidate gene cluster, the previously published sequences of the BGCs encoding azaphilones in

Monascus ruber^[20] (i.e., monascin, ankaflavin, and monascorubrin), azanigerones in *Aspergillus niger*,^[21] and mitorubrinol in *Talaromyces marneffei*^[22] were used for homology searches. In *M. ruber*, *A. niger*, and *T. marneffei* assembly of the azaphilone core structure is initiated by the action of a non-reducing polyketide synthase (NR-PKS) and finalized by subsequent processing of a ketoreductase (KR) and FAD-dependent monooxygenase (FAD-MO).^[20] These three core proteins were initially used as the template for BLASTP searches against a *H. fragiforme* protein database created by using the software Geneious 9.1.8.

In total, seven NR-PKS-containing BGCs were found. However, only one included the required KR and FAD-MO encoding genes. This BGC (designated *hfaza1*, GenBank Acc. No. MN736721) is composed of seven genes, the majority of which show high homology with the biosynthetic genes of the *M. ruber* azaphilone *mrPig* and the *T. marneffei* mitorubrinol BGCs (Figure 3). In addition to the NR-PKS (*hfaza1A*), the KR (*hfaza1F*), and the FAD-MO (*hfaza1D*), genes encoding an

Table 2. ^{13}C NMR spectroscopic data [ppm] of hybridorubrins A–D (1–4) and fragirubrins F–G (5–6) (1, 3–4, 6: 175 MHz; 2, 5: 125 MHz).

Position	1 ^[a]	2 ^[b]	3 ^[a]	4 ^[a]	5 ^[a]	6 ^[b]
1	65.0, CH ₂	64.5, CH ₂	65.0, CH ₂	64.9, CH ₂	155.0, CH	153.7, CH
3	166.1, C	165.4, C	166.2, C	167.9, C	159.3, C	157.8, C
4	98.3, CH	96.5, CH	98.3, CH	97.7, CH	111.3, CH	110.8, CH
5	143.4, C	142.1, C	143.4, C	143.6, C	143.1, C	141.9, C
6	129.6, C	129.2, C	129.6, C	129.8, C	107.6, CH	107.5, CH
7	194.6, C	193.8, C	194.6, C	194.6, C	192.6, C	192.8, C
8	85.7, C	84.5, C	85.7, C	85.7, C	85.4, C	84.1, C
9	189.7, C	189.1, C	189.7, C	189.6, C	193.8, C	193.2, C
10	115.6, C ^[c]	115.2, C	115.6, C	115.4, C	116.0, C	115.2, C
11	22.6, CH ₃	22.1, CH ₃	22.6, CH ₃	22.6, CH ₃	22.7, CH ₃	22.1, CH ₃
12	41.5, CH ₂	40.9, CH ₂	41.5, CH ₂	45.4, CH ₂	39.9, CH ₂	39.4, CH ₂
13	68.8, CH	68.2, CH	68.8, CH	45.4, CH ₂	68.4, CH	67.5, CH
14	20.4, CH ₃	20.2, CH ₃	20.4, CH ₃	24.0, CH ₃	20.0, CH ₃	19.9, CH ₃
15	170.6, C	170.6, C	170.6, C	–	170.5, C	170.2, C
16	21.2, CH ₃	21.3, CH ₃	21.2, CH ₃	–	21.1, CH ₃	21.2, CH ₃
1'	172.4, C	172.5, C	172.4, C	172.4, C	172.7, C	173.1, C
2'	33.9, CH ₂	33.2, CH ₂	33.9, CH ₂	33.9, CH ₂	33.8, CH ₂	33.2, CH ₂
3'	25.6, CH ₂	24.6, CH ₂	25.6, CH ₂	25.6, CH ₂	25.6, CH ₂	24.6, CH ₂
4'	29.8, CH ₂	28.9, CH ₂	29.9, CH ₂	29.5, CH ₂	29.7, CH ₂	28.9, CH ₂
5'–7'	30.4, CH ₂ ^[c]	29.1, CH ₂ ^[c]	30.1, CH ₂ ^[c]	30.4, CH ₂ ^[c]	29.8, CH ₂ ^[c]	29.2, CH ₂ ^[c]
8'	30.4, CH ₂ ^[c]	27.2, CH ₂	27.9, CH ₂ ^[c]	30.4, CH ₂ ^[c]	30.4, CH ₂ ^[c]	27.2, CH ₂ ^[c]
9'	30.4, CH ₂ ^[c]	130.3, CH	130.6, CH ^[c]	30.4, CH ₂ ^[c]	30.4, CH ₂ ^[c]	129.9, CH ^[c]
10'	30.4, CH ₂ ^[c]	127.8, CH	130.6, CH ^[c]	30.4, CH ₂ ^[c]	30.4, CH ₂ ^[c]	129.9, CH ^[c]
11'	26.6, CH ₂	25.6, CH ₂	27.9, CH ₂ ^[c]	30.4, CH ₂ ^[c]	30.4, CH ₂ ^[c]	27.2, CH ₂ ^[c]
12'	38.7, CH ₂	128.6, CH	30.1, CH ₂ ^[c]	30.4, CH ₂ ^[c]	26.6, CH ₂	29.2, CH ₂ ^[c]
13'	71.2, CH	129.5, CH	30.1, CH ₂ ^[c]	30.4, CH ₂ ^[c]	38.1, CH ₂	29.2, CH ₂ ^[c]
14'	40.9, CH ₂	23.6, CH ₂	30.1, CH ₂ ^[c]	32.7, CH ₂	72.9, CH	31.8, CH ₂
15'	19.7, CH ₂	23.6, CH ₂	26.7, CH ₂	23.4, CH ₂	31.2, CH ₂	22.6, CH ₂
16'	14.6, CH ₃	36.6, CH ₂	40.4, CH ₂	14.4, CH ₃	10.5, CH ₃	14.1, CH ₃
17'	–	72.9, CH	67.6, CH	–	–	–
18'	–	30.2, CH ₂	24.2, CH ₃	–	–	–
1a	155.2, CH	153.8, CH	155.4, CH	155.2, CH	–	–
3a	155.4, C	154.4, C	155.2, C	155.5, C	–	–
4a	115.8, CH	114.7, CH	115.8, CH	115.7, CH	–	–
5a	143.0, C	141.9, C	143.0, C	143.1, C	–	–
6a	110.0, CH	109.5, CH	110.0, CH	109.9, CH	–	–
7a	192.3, C	192.6, C	192.3, C	192.3, C	–	–
8a	86.8, C	84.9, C	86.8, C	86.8, C	–	–
9a	192.8, C	192.2, C	192.8, C	192.8, C	–	–
10a	115.6, C ^[c]	114.5, C	115.6, C	115.6, C	–	–
11a	22.7, CH ₃	22.2, CH ₃	22.7, CH ₃	22.7, CH ₃	–	–
12a	135.1, CH	132.9, CH	135.1, CH	135.0, CH	–	–
13a	131.5, CH	131.1, CH	131.5, CH	131.5, CH	–	–
14a	140.2, CH	137.9, CH	140.2, CH	140.0, CH	–	–
1a'	105.0, C	104.5, C	105.0, C	105.0, C	–	–
2a'	166.2, C	165.5, C	164.0, C	166.2, C	–	–
3a'	101.8, CH	101.1, CH	101.8, CH	101.8, CH	–	–
4a'	164.0, C	161.5, C	166.2, C	164.0, C	–	–
5a'	112.7, CH	111.7, CH	112.7, CH	112.7, CH	–	–
6a'	144.9, C	144.7, C	144.9, C	144.9, C	–	–
7a'	24.1, CH ₃	24.0, CH ₃	24.1, CH ₃	24.1, CH ₃	–	–
8a'	170.7, C	169.9, C	170.7, C	170.7, C	–	–

[a] [D₆]acetone. [b] CDCl₃. [c] Signals could not be unambiguously assigned due to overlap.

NADPH-dependent dehydrogenase (*hfaza1B*), an ac(et)yltransferase (*hfaza1E*), a transporter (*hfaza1C*), and a transcription factor (*hfaza1G*) are present.

A previous investigation of the mitorubrinol gene cluster in *T. marneffeii* showed that two PKS genes are involved in the biosynthesis of **8** and **10**.^[22] The second PKS encodes the biosynthesis of orsellinic acid. We therefore searched for a homologue of the putative *T. marneffeii* orsellinic acid synthase

(OSAS) *pks12* in *H. fragiforme*. Accordingly, we found a gene cluster encoding a highly similar NR-PKS together with a set of genes of which the majority also appeared in the *M. ruber* (Figure 3) and *A. niger* azaphilone BGCs. This second gene cluster is designated *hfaza2* (GenBank Acc. No. MN736720). The respective NR-PKS (*Hfaza2A*) has an SAT-KS-AT-PT-ACP domain structure, and thus lacks a typical C-terminal release domain. Additional genes in the *hfaza2* BGC encode an FAD-MO

Table 3. Inhibitory effect of azaphilones from *Hypoxylon fragiforme* on biofilm formation of *Staphylococcus aureus*.

Compound	Biofilm inhibition [%] ^[a]	Concentration [$\mu\text{g} \times \text{mL}^{-1}$]	Potency of inhibition ^[b]
hybridorubrin A (1)	81	250	+++
	72	125	
	68	62.5	
	61	31.3	
	45	15.6	
	32	7.8	
	27	3.9	
hybridorubrin C (3)	82	250	+++
	79	125	
	65	62.5	
	60	31.3	
	60	15.6	
	34	7.8	
	25	3.9	
hybridorubrin D (4)	71	250	+++
	61	125	
	50	62.5	
	37	31.3	
	27	15.6	
mitorubrin (7)	29	250	+
	27	125	
	27	62.5	
mitorubrinol (8)	n.i.	250	–
mitorubrinol acetate (9)	24	250	+
mitorubrinic acid (10)	n.i.	250	–
rutilin C (12)	59	250	+++
	72	125	
	63	62.5	
	51	31.3	
	41	15.6	
lenormandin F (14)	n.i.	250	–
fragirubrin A (15)	27	250	+
	29	125	
	38	62.5	
microporenic acid A ^[19]	81	250	+++
	83	125	
	45	62.5	
	20	31.3	

[a] Only inhibition values $\geq 20\%$ are listed here; n.i.: no inhibition. [b] + + +: inhibition $\geq 70\%$; + +: inhibition ≥ 40 and $< 70\%$; +: inhibition ≥ 20 and $< 40\%$; –: inhibition $< 20\%$.

(*hfaza2D*) with high homology to *hfaza1D* and *mrPigN*, an ac(etyl)transferase (*hfaza2E*) homologous to *hfaza1E* and *mrPigD*, a P450 monooxygenase (*hfaza2F*), and an NADPH-dependent dehydrogenase (*hfaza2L*) with homology to *hfaza1B* and *mrPigH*. Furthermore, two similar genes were also found in the BGC (*hfaza2B* and *hfaza2C*) that did not produce any hits in BLASTP searches against the Swiss-Prot database, but showed strong homology with the azaphilone biosynthesis genes *mrPigM* and *mrPigO* from *M. ruber*. On the basis of knockout experiments of the latter two, it was deduced that *MrPigM* is an acetyltransferase, whereas *MrPigO* performs deacetylation.^[20] In addition to these genes, two FAD-dependent oxidoreductases (*hfaza2J* and *hfaza2M*) were found, which are very similar to *azaG* and *azaL*, both of which are part of the azanigerone biosynthetic pathway.^[21]

Finally, two putative transcription factors (*hfaza2G* and *hfaza2H*) and two putative transporters (*hfaza2I* and *hfaza2K*)

were also assigned to the cluster. A detailed comparison of the *hfaza1* and *hfaza2* clusters with the uncharacterized mitorubrinol BGC reported from *T. marneffe*^[22] showed the presence of almost all genes from the latter in the *H. fragiforme* BGC (Figure 3). Homologues of *Hfaza1A*, *Hfaza2A*, *Hfaza1B*, *Hfaza2B*, *Hfaza2C*, *Hfaza1E*, *Hfaza2E*, *Hfaza1F*, and *Hfaza2L*, were found. The *T. marneffe* cluster is expanded by two hydrolase enzymes, but no FAD-dependent monooxygenase, P450 monooxygenases, FAD-dependent oxidoreductases, and transcription factors are present. Therefore, we propose, according to the homology analyses, that two unlinked BGCs (*hfaza1* and *hfaza2*) act together to assemble and diversify azaphilones in *H. fragiforme*.

H. fragiforme does not readily produce azaphilones in laboratory culture, so it is not yet possible to investigate the biosynthesis experimentally. However, there is now sufficient detailed knowledge concerning the biosynthesis of related compounds in other organisms to allow the development of a detailed biosynthetic hypothesis based on the combination of structure information and analytical HPLC-MS data (Scheme 1).

The formation of azaphilones likely starts in a similar fashion as proved for azanigerones and *Monascus* pigments with the NR-PKS *Hfaza1A* producing a hexaketide chain, which is subsequently cyclised by the product template (PT) domain and released by the reductive release (R) domain of the PKS to yield the reactive benzaldehyde intermediate **20**. Chen et al. reported that in *M. ruber* ketoreduction at C-13 is required prior to hydroxylation at C-8 to afford the pyran ring.^[20] In the crude stromatal extracts of *H. fragiforme* we could not find any evidence for the existence of such a bicyclic pyranoquinone intermediate **22**. Instead, we found a conspicuous peak with $m/z = 249 [M+H]^+$, which showed fragmentation patterns, a UV/Vis spectrum, and molecular formula consistent with the putative keto intermediate **21** (Tables S4, S5 in the Supporting Information). We therefore conclude that **21** might be produced by hydroxylation of **20** at C-8 by the FAD-MO *Hfaza1D* and subsequent spontaneous pyran ring formation. As *Hfaza2D* also encodes a homologous enzyme, it is possible that it can perform the same reaction. In a previous study based on crystal structure data and quantum mechanical/molecular mechanical calculations of the homologous FAD-MO TropB, it has been demonstrated that such enzymes govern a highly enantioselective transformation.^[23] The occurrence of the homologous pair *Hfaza1D/Hfaza2D* would therefore be consistent with the observation of different stereoconfigurations at C-8 between mitorubrin-type and fragirubrin-type azaphilones. Compound **21** can then be further processed by the ketoreductase *Hfaza1F* to yield **22**. As previously stated, we could not detect **22**, which can possibly be explained by differences in metabolic rates due to differences in enzyme reaction rates or expression levels of *hfaza1F* and subsequent processing enzymes.

In the next step, the pathway branches into two directions depending on the attached side chain. In order to yield lenormandin-type azaphilones such as **14**, the backbone **22** can undergo acylation at the C-8 alcohol mediated by the acyltransferase *Hfaza1E*. Subsequent acetylation at the C-13 alcohol by the putative acetyltransferase *Hfaza2B* will lead to the highly

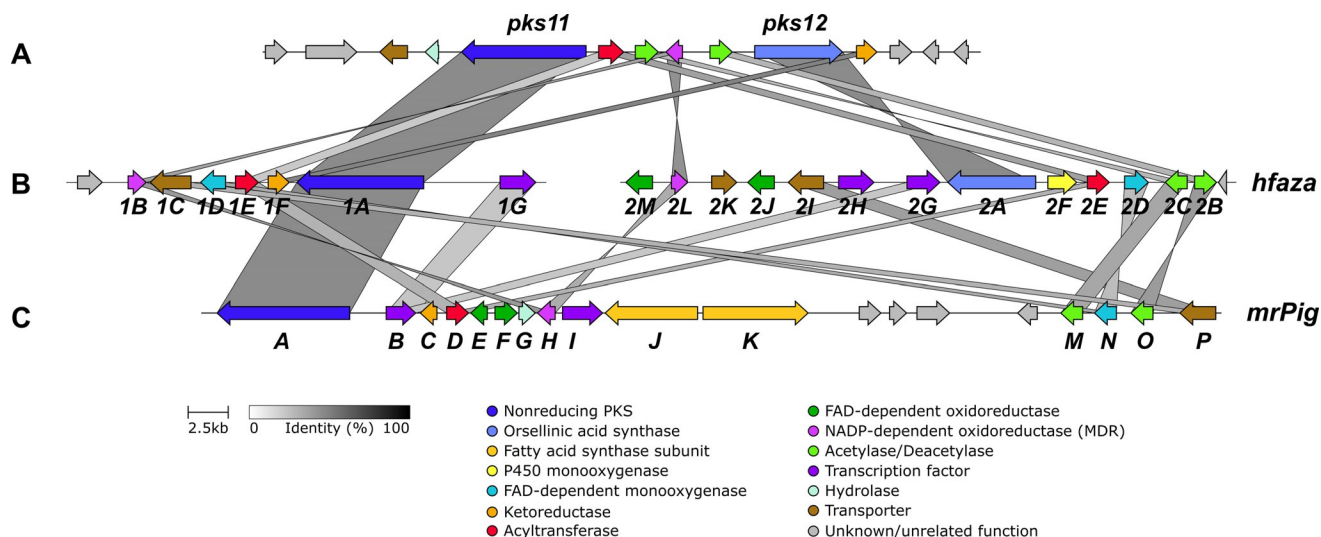
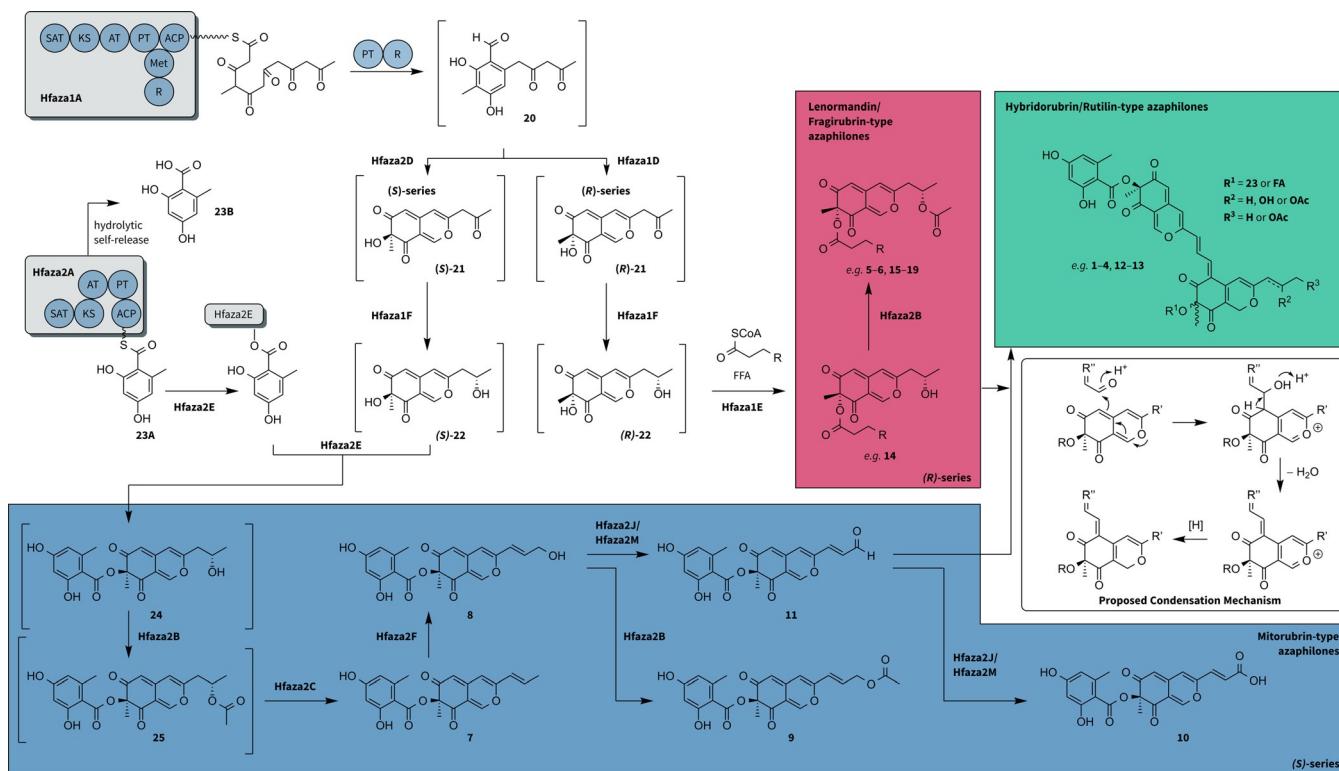


Figure 3. Gene cluster comparison of the BGCs encoding for azaphilone production visualized with the clinker tool: **A**, the known mitorubrin BGC of *T. marneffei*; **B**, *hfaza1* and *hfaza2* from *H. fragiforme*; **C**, the known *mrPig* BGC from *M. ruber*. In accordance with the original publication,^[22] no further labels were assigned to the *T. marneffei* genes.



Scheme 1. Biosynthetic hypothesis for the production and diversification of azaphilone-type compounds in *H. fragiforme*. Putative intermediates that could not be isolated and were only detectable in traces by HPLC-MS or not detectable at all are shown in square brackets. R in the free fatty acids (FFA) and respective side chain indicates variations in chain length, hydroxylation and unsaturation pattern depending on the final product.

diverse group of fragirubrins (5–6, 15–19), which differ among each other in the chain length, desaturation level, and hydroxylation pattern of the side chain. This side chain very likely originates from different free or CoA-bound fatty acids of the primary metabolism implying a broad substrate tolerance of Hfaza1E. Acyltransferases accepting a wide range of enzyme-

free acyl substrates are also involved in the biosynthesis of squalastatin.^[24] As only lenormandin F (14) has been isolated as a representative of this type of compounds from *H. fragiforme*, we assume that the majority of lenormandins are transformed into the respective fragirubrins. This hypothesis is consistent with observations made in *H. lenormandii*, which only

produces the azaphilones named after this fungus.^[12] Thus, it can be speculated that *H. lenormandii* lacks homologues of Hfaza2B.

The diversity of mitorubrin-type azaphilones likely starts by the attachment of orsellinic acid (**23**) to the hydroxyl group at C-8 catalysed by Hfaza2E leading to the intermediate **24**. Due to the structural differences between **23** and fatty acids, it seems unlikely that transfer reactions are conducted by the very same enzyme. Hence, we expect the acyltransferases from both clusters to be specific for different types of substrates. In addition, we assume that these enzymes are also highly stereoselective concerning the substrate **22**, as only a single enantiomer for each compound can be detected.

Due to the absence of another obvious OSAS encoded in the genome, the involvement of Hfaza2A in the synthesis of **23** seems most likely. This is also supported by the strong homology of Hfaza2A to PKS12 of the mitorubrinol BGC in *T. marneffeii*. The latter enzyme was shown to be crucial for mitorubrinol **8**^[25] and mitorubrinic acid **10**^[25] biosynthesis by knockdown experiments in the producing fungus, but the actual function could not be deduced from the data. Hence, it was speculated that PKS12 might be responsible for orsellinic acid biosynthesis. Unfortunately, the authors only looked specifically for the absence of **8** and **10**, but did not search for additional products in the extracts of their transformants to confirm this idea.^[22]

The lack of a release domain in the proposed OSAS Hfaza2A could be compensated by the acyltransferase Hfaza2E, which might directly load the ACP-bound **23A**. Such a reaction has already been suggested for the acyltransferase MrPigD, which presumably accepts ACP-bound fatty acids in *Monascus* pigment biosynthesis^[20] and has been well characterised for the acyltransferase LovD involved in lovastatin biosynthesis.^[26] Because **23B** can also be detected as free acid in the stromatal crude extracts, we expect a hydrolytic self-release mechanism analogously to truncated forms of the methylorcinolaldehyde synthase.^[27] Intermediate **24** is then acetylated by the putative acetyl transferase Hfaza2B to give **25**. Mass searches for compounds **24** and **25** revealed the presence of respective traces in the stromatal crude extracts (Table S5 in the Supporting Information). Because of the very small amount of compound the corresponding relationships can, however, not be verified. The following step might involve deacetylation carried out by Hfaza2C to yield mitorubrin (**7**), which in return is hydroxylated at C-14 putatively by the P450 monooxygenase Hfaza2F to afford one of the major stromatal metabolites, mitorubrinol (**8**).

Mitorubrinol (**8**) then acts as the starting material for the biosynthesis of **9** through the acetylation of the C-14 alcohol performed either by Hfaza2B or a cluster-independent acetyltransferase. In addition, **8** is also likely to be an intermediate towards mitorubrinic acid (**10**) via formation of the aldehyde mitorubrinol (**11**). We found a corresponding peak in stromatal crude extracts exhibiting the expected mass spectra (Figure S2, Tables S4, S5 in the Supporting Information). We were unable to isolate this compound, but standards of **11** obtained semi-synthetically by oxidation of **8** with manganese oxide proved that the observed peak indeed corresponds to **11**.

The respective biosynthetic steps to **10** might be carried out by the action of the FAD-dependent oxidoreductases Hfaza2J and Hfaza2M. As the *T. marneffeii* BGC also encodes the production of **10**, but lacks oxidoreductase genes, a different mechanism is also possible. Interestingly, the mitorubrinol cluster of *T. marneffeii* only leaves limited options to explain the conversion of **11** to **10**. The function of the highly conserved NADPH-dependent dehydrogenase still remains obscure in all azaphilone biosynthetic pathways. Hence, it could theoretically also be involved in such oxidation steps.

Finally, we propose that the aldehyde functionality of **11** acts as an electrophile for the nucleophilic C-6 in all *H. fragiforme* monomeric azaphilones to afford dimers of the rutilin- (**12–13**) and hybridorubrin-type (**1–4**), as already postulated by Quang et al. for rutilins A and B.^[28] The presence of rutilins in *Hypoxylon rutilum* as major stromatal metabolites could also indicate that condensation is enzyme-catalysed.^[28] However, this phenomenon could also be explained by the lack of an FAD-dependent oxidoreductase to prevent the biosynthesis of a carboxylic acid functionality and leave the reactive aldehyde as the final enzymatic product. This is also consistent with the observation that no carboxylated azaphilones have been detected in *H. rutilum*.^[28] On the other hand, the mechanism could also involve radicals. The structures of the known bis-azaphilone diazaphilonic acid^[29] or the azaphilone-derived nitrogen-containing chaetoglobins^[30] (Figure S3 in the Supporting Information) might possibly be formed by recombination of radicals establishing the carbon–carbon bond connecting the substructures.

When comparing the biosynthetic machinery of mitorubrins in *H. fragiforme* and *T. marneffeii* various questions remain. The lack of monooxygenase genes in the cluster of the latter would prevent backbone assembly. Furthermore, monooxygenases are also very likely required to obtain mitorubrinol (**8**). Therefore, it seems likely that enzymes encoded outside of the BGC participate in the azaphilone formation of *T. marneffeii*. Based on our biosynthetic hypothesis, we propose that the production of lenormandin-type azaphilones requires only genes from *hfaza1* and thus is likely evolved earlier in these fungi. Consequently, *hfaza2* might be acquired later, for example, by horizontal gene transfer from *T. marneffeii* or related fungi and has proved for the fungus to be compatible with *hfaza1*.

The existence of intertwining secondary metabolite gene clusters has already been reported for the production of the structurally distant compounds fumagillin and pseurotin A in *Aspergillus fumigatus*.^[25] However, these clusters were physically linked and consequently translocation of genes into neighbouring BGC can be explained by simple inversion of certain genomic regions within such a supercluster. Recently, independent gene clusters have been demonstrated to be responsible for the formation of the azaphilone azasperpyranone A in *Aspergillus terreus*. While one BGC produced the azaphilone backbone, the other BGC afforded and processed 5-methyl orsellinic acid (5-MOA). The respective 5-MOA PKS contained a methyltransferase and thioesterase domain and shared only little homology with Hfaza2A.

In addition to the elucidation of the biosynthetic pathway of azasperpyranon A, the regulatory network of the participating BGCs was deciphered by gene knockout of the encoded transcription factors (TF) and gene expression analysis. It was shown that each BGC is upregulated by a cluster-specific TF, which in return are regulated by a third TF located in one of the BGCs.^[31] The regulatory network for azaphilone production in *H. fragiforme* could be highly similar, as three TFs have been identified across *hfaza1* and *hfaza2*. We thus tried to experimentally link *hfaza1* and *hfaza2* with the known azaphilones by ectopic overexpression of the individual TF genes using previously described methods.^[32] However, this proved unsuccessful. Knockout strategies are not viable in the Hypoxylaceae, as azaphilones are exclusively formed during stomatal development, which cannot be induced under laboratory conditions.

We could also find highly similar homologues of the two clusters in the taxonomically related fungus *H. rickii* and the more distantly related *H. rubiginosum* (data not shown), which are known to produce mitorubins and/or the closely-related rubiginosins.^[33] This observation further supports our theory about azaphilone biosynthesis in *H. fragiforme* and enables further options to study the pathways in detail. However, it will be a special challenge to obtain final proof of the biosynthetic mechanism, because the stomata can presently not be grown in the laboratory, and hence the only path forward would be heterologous expression.

Conclusion

We used a combination of classical natural product chemistry and state-of-the-art genome sequencing to deduce the biosynthesis of azaphilone pigments in *H. fragiforme*, demonstrating the powerful combination of those two methods. We showed that both possible C-8 stereoisomers of azaphilones are produced in the stomata, which allows for assignment to subgroups: 1) the C-8(R)-configured azaphilones consist of the acyl-carrying lenormandins and fragirubins; 2) the group of C-8(S)-configured azaphilones carry an orsellinic acid moiety and belong to the family of mitorubins and their fusion products, rutilins; and 3) the novel hybridorubins, which are of mixed stereochemistry, as their building blocks originate from groups 1 and 2. Furthermore, the hybridorubins A (1), C (3), and D (4) exhibited high bioactivity against formation of *S. aureus* biofilms.

Examination of the *H. fragiforme* genome revealed two BGCs to be most likely responsible for biosynthesis of azaphilone polyketides. The *hfaza1* BGC is likely responsible for biosynthesis of the azaphilone backbone and addition of fatty acid moieties to yield group 1 compounds. In parallel, the *hfaza2* BGC synthesizes orsellinic acid, which is esterified to the backbone to yield group 2 azaphilones and tailors the gained mitorubins to obtain a high diversity of derivatives. We suggest that a spontaneous aldol condensation reaction is responsible for the formation of hybridorubrin and rutilin bis-azaphilones from reactive aldehyde intermediates in *H. fragiforme*; however, this needs experimental verification. These results reveal the first

example of two distant, cross-acting BGCs that enable a large diversity of azaphilone products through natural mix-and-match strategies.

Experimental Section

General

NMR spectra were recorded with an Avance III 700 spectrometer with a 5 mm TCI cryoprobe (¹H 700 MHz, ¹³C 175 MHz) and an Avance III 500 spectrometer (¹H 500 MHz, ¹³C 125 MHz) (both Bruker, Billerica, MA/USA). Optical rotations were taken with a MCP 150 polarimeter (Anton Paar, Graz, Austria) and UV spectra with a UV-2450 UV/Vis spectrophotometer (Shimadzu, Kyoto, Japan). IR spectra were taken with a Spectrum 100 FTIR spectrometer (Perkin Elmer, Waltham, MA/USA) and ECD spectra were measured using a J-815 spectropolarimeter (Jasco, Pfungstadt, Germany).

ESI mass spectra were recorded with an UltiMate 3000 Series uHPLC (Thermo Fisher Scientific, Waltham, MA/USA) by utilizing a C18 Acquity UPLC BEH column (50×2.1 mm, 1.7 μm; Waters, Milford, USA) connected to an amaZon speed ESI-Iontrap-MS (Bruker, Billerica, MA, USA). HPLC parameters were set as follows: solvent A: H₂O + 0.1% formic acid, solvent B: acetonitrile (MeCN) + 0.1% formic acid, gradient: 5% B for 0.5 min, increasing to 100% B over 19.5 min, keeping 100% B for a further 5 min, flow rate 0.6 mL min⁻¹, and DAD detection 190–600 nm.

ESI-HRMS was performed with an Agilent 1200 Infinity Series HPLC (Agilent Technologies, Böblingen, Germany; conditions as for ESI-MS) connected to a maXis ESI-TOF-MS (Bruker).

Fungal material and extraction

To generate crude extract 1 air-dried stomata (fruiting bodies, ca. 65 g) of *Hypoxylon fragiforme* were collected in 2017 from *Fagus sylvatica* in the vicinity of Braunschweig, Germany, by Lucile Wendt. Extraction was performed by adding 500 mL of acetone, followed by ultrasonication at 40 °C for 1 h. This procedure was repeated twice. The extracts were combined and dried in vacuo, which led to approximately 6 g of crude extract 1. For crude extract 2, about 25 g of air-dried stomata of *Hypoxylon fragiforme* were collected in 2016 from *Fagus sylvatica* in the vicinity of Lake Starnberg, Germany, by Lucile Wendt. Extraction was performed as described above. This yielded approximately 3 g of crude extract 2.

Isolation of secondary metabolites 1–6

Crude extract 1 yielded hybridorubins A, B (1, 2) and fragirubins F, G (5 and 6), while hybridorubins C, D (3, 4) could be detected but not isolated to purity. Thus, extract 2 was utilised to isolate 3 and 4, while 1 was isolated again as a by-product.

Initially, crude extract 1 was separated by a Reveleris X2 Flash Chromatography system (Büchi, Essen, Germany). A 40 g silica cartridge (120×30 mm, 40 μm, SN 145146132, W.R. Grace, Columbia, MD/USA) was loaded with the crude extract and eluted with a ternary gradient (solvent A: CH₂Cl₂, B: CH₂Cl₂:acetone 9:1, C: acetone) as follows: at a flow rate of 40 mL min⁻¹, isocratic conditions at 100% A were set for 4 min, followed by a gradient to 100% B over 25 min. This was followed by an increase of solvent C to 100% over 20 min. This led to six fractions (t_R fraction I: 3.4–14.3 min, II: 14.7–15.9 min, III: 16.6–20.4 min, IV: 21–25.4 min, V: 26–29.8 min, VI: 30.3–52.2 min), which were evaporated to dryness in vacuo at 40 °C.

Fractions I, II, and V (see below) were further processed by using a preparative HPLC system (Gilson, Middleton, WI/USA; GX-271 Liquid Handler with a GX Direct Injection Module, DAD 172, 305 and 306 Pump, 806 Manometric Module 811D Dynamic Mixer, 402 Syringe Pump). A Nucleodur C18ec column (150×40 mm, 7 μm; Macherey-Nagel, Düren, Germany) was used at a flow rate of 40 mL min⁻¹ with solvent A: H₂O + 0.1% formic acid and solvent B: MeCN + 0.1% formic acid. After evaporation of MeCN in vacuo, the aqueous residues were frozen and freeze-dried with an Alpha 1–4 LSC freeze dryer (Christ, Osterode, Germany). Fractions I (2×70 mg) and II (3×100 mg) were separated with a gradient under isocratic conditions for 5 min at 60% B, followed by an increase to 100% B over 45 min, 5 min of isocratic conditions, and, ultimately, a decrease to 60% B over 2 min. Fragarubrin G (**6**, 0.9 mg) was gained from fraction I, while fragarubrin F (**5**, 21.6 mg) was isolated from fraction II. Fraction V (1×100 mg) was separated by using a gradient from 45 to 80% B over 40 min, followed by an increase to 100% B over 5 min and isocratic conditions at 100% B for 15 min. It yielded hybridorubrin B (**2**, 2.8 mg). Fraction VI (1×40 mg) was separated with an RP-MPLC system (Kronlab, Sinsheim, Germany; column 480×30 mm, ODS/AQ C18, solvents as described for fractions I–V) at a flow rate of 30 mL min⁻¹. Starting with isocratic conditions at 10% B for 5 min, a gradient to 100% B over 60 min was followed by isocratic conditions at 100% B for 30 min. Hybridorubrin A (**1**, 4.1 mg) was obtained from this separation.

Crude extract 2 was separated by using the aforementioned Reveleris X2 flash chromatography system. A 120 g C18 cartridge (200×40 mm, 40 μm, SN 5152991, Grace) was loaded with the crude extract and eluted with a binary gradient (solvent A: H₂O + 0.1% formic acid; solvent B: MeCN + 0.1% formic acid) as follows: flow rate: 80 mL min⁻¹, isocratic conditions at 5% B for 3 min, followed by an increase to 45% B over 1 min. This was followed by an increase to 80% B over 10 min. Subsequently, the gradient was increased to 100% B over 25 min. This was kept for a further 20 min. This yielded fractions I (*t_R*: 40–45 min) and II (52.5–70 min). Both fractions I (1×180.3 mg) and II (1×122 mg), were individually processed by manual NP column chromatography. For this, the material was adsorbed on silica bulk material (63–200 μm) and transferred to a loading cartridge (SN 8634349, Grace). Downstream of that, a 12 g silica cartridge (SN 5146131, Grace) was installed. Under a vacuum of approximately 50 mbar, the extract was separated by using the following solvents: A: *n*-heptane, B: CH₂Cl₂, C: MeOH. A step gradient with 100 mL of the following solvent mixtures was gradually applied: i) 20:80:0 (% A:B:C, v/v/v), ii) 0:100:0, iii) 0:99:1, iv) 0:98:2, v) 0:96:4, vi) 0:93:7, vii) 0:90:10, viii) 0:85:15, ix) 0:80:20. Each solvent mixture was loaded onto the device and the eluent gathered before another step was applied. Thus, chromatographic separation of fraction I yielded fraction v, while fraction II yielded fractions vi and vii, which were combined. Fraction v (2×10.5 mg) was further separated with a PLC 2250 HPLC system (Gilson) equipped with an X-Bridge C18 column (250×19 mm, 5 μm, Waters), solvents A: H₂O + 0.1% formic acid and B: MeCN + 0.1% formic acid, and the following gradient: flow rate: 20 mL min⁻¹, isocratic conditions at 40% B for 5 min, followed by an increase to 75% B over 5 min. This was followed by an increase to 100% B over 50 min. This yielded hybridorubrin D (**4**, 1.7 mg). Fraction vi+vi (8×11 mg) was separated by using the PLC 2250 with the conditions as described above. First, isocratic conditions at 40% B were applied for 5 min, followed by an increase to 75% B over 5 min. Then, 75% B was kept for 25 min. The same fractions of the eight separations were combined according to LCMS results, which yielded hybridorubrin A (**1**, 11.9 mg) and a yet-impure hybridorubrin C (**3**). The latter (1×4.7 mg) was further

purified by again using the PLC 2250 under the same conditions as before, but with the exception of applying 77% instead of 75% B. This yielded hybridorubrin C (**3**, 1.7 mg).

Physicochemical data

Hybridorubrin A (**1**): red oil; $[\alpha]_D = +340$ (*c* = 0.02, MeCN); ¹H NMR ([D₆]acetone, 700 MHz): see Table 1; ¹³C NMR ([D₆]acetone, 175 MHz): see Table 2; IR (ATR): $\tilde{\nu}_{\max} = 2927, 2854, 1717, 1621, 1261$ cm⁻¹, see Figure S42 in the Supporting Information; UV/Vis (acetone): $\lambda_{\max} (\epsilon) = 215$ (4.54), 268 (4.40), 360 (4.60), 441 (4.37) nm; ECD (MeCN) $\lambda(\Delta\epsilon) = 231$ (−5.0), 265 (−0.6), 293 (−5.4), 360 (+5.3) nm, see Figure S43 in the Supporting Information; ESI-MS: *m/z* 927.58 [M+H]⁺, 925.55 [M−H][−]; HR-ESI-MS: *m/z* 927.4163 [M+H]⁺ (calcd for C₅₂H₆₃O₁₅: 927.4161); *t_R* = 16.3 min.

Hybridorubrin B (**2**): red oil; $[\alpha]_D = +580$ (*c* = 0.02, MeCN); ¹H NMR (CDCl₃, 500 MHz): see Table 1; ¹³C NMR (CDCl₃, 125 MHz): see Table 2; IR (ATR): $\tilde{\nu}_{\max} = 2929, 2855, 1717, 1630, 1263$ cm⁻¹, see Figure S42; UV/Vis (MeCN): $\lambda_{\max} (\epsilon) = 213$ (4.50), 268 (4.37), 362 (4.52), 441 (4.31) nm; ECD (MeCN) $\lambda(\Delta\epsilon) = 198$ (+5.4), 231 (−8.9), 267 (−1.7), 290 (−8.7), 355 (+8.0) nm, see Figure S43 in the Supporting Information; ESI-MS: *m/z* 951.49 [M+H]⁺, 949.48 [M−H][−]; HR-ESI-MS: *m/z* 951.4154 [M+H]⁺ (calcd for C₅₄H₆₃O₁₅: 951.4161); *t_R* = 16.4 min.

Hybridorubrin C (**3**): red oil; $[\alpha]_D = +355$ (*c* = 0.02, MeCN); ¹H NMR ([D₆]acetone, 700 MHz): see Table 1; ¹³C NMR ([D₆]acetone, 175 MHz): see Table 2; IR (ATR): $\tilde{\nu}_{\max} = 2930, 2855, 1717, 1630, 1263$ cm⁻¹, see Figure S42 in the Supporting Information; UV/Vis (MeCN): $\lambda_{\max} (\epsilon) = 215$ (4.4), 269 (4.2), 364 (4.4), 443 (4.1) nm; ECD (MeCN) $\lambda(\Delta\epsilon) = 197$ (−7.2), 206 (−3.1), 213 (−8.3), 218 (−2.2), 232 (−12.7), 267 (+1.7), 289 (−11.0), 352 (+8.9) nm, see Figure S43 in the Supporting Information; ESI-MS: *m/z* 953.52 [M+H]⁺, 951.48 [M−H][−]; HR-ESI-MS: *m/z* 953.4321 [M+H]⁺ (calcd for C₅₄H₆₅O₁₅: 953.4318); *t_R* = 16.6 min.

Hybridorubrin D (**4**): red oil; $[\alpha]_D = +173$ (*c* = 0.015, MeCN); ¹H NMR ([D₆]acetone, 700 MHz): see Table 1; ¹³C NMR ([D₆]acetone, 175 MHz): see Table 2; IR (ATR): $\tilde{\nu}_{\max} = 2924, 2854, 1721, 1622, 1262$ cm⁻¹, see Figure S42; UV/Vis (MeCN): $\lambda_{\max} (\epsilon) = 214$ (4.36), 266 (4.11), 337 (4.12) nm; ECD (MeCN) $\lambda(\Delta\epsilon) = 209$ (+2.6), 228 (−2.4), 268 (−0.5), 296 (−4.5), 330 (+2.7) nm, see Figure S43 in the Supporting Information; ESI-MS: *m/z* 869.43 [M+H]⁺, 867.39 [M−H][−]; HR-ESI-MS: *m/z* 869.4110 [M+H]⁺ (calcd for C₅₀H₆₀O₁₃: 869.4107); *t_R* = 18.7 min.

Fragarubrin F (**5**): yellow oil; $[\alpha]_D = -10$ (*c* = 0.1, MeCN); ¹H NMR ([D₆]acetone, 500 MHz): see Table 1; ¹³C NMR ([D₆]acetone, 125 MHz): see Table 2; IR (ATR): $\tilde{\nu}_{\max} = 2925, 2854, 1737, 1715, 1639, 1233$ cm⁻¹, see Figure S42 in the Supporting Information; UV/Vis (MeCN): $\lambda_{\max} (\epsilon) = 220$ (4.18), 326 (4.22) nm; ECD (MeCN) $\lambda(\Delta\epsilon) = 199$ (−8.1), 232 (+1.9), 248 (−1.6), 273 (+5.2), 323 (−5.3) nm, see Figure S44 in the Supporting Information; ESI-MS: *m/z* 547.34 [M+H]⁺, 545.28 [M−H][−]; HR-ESI-MS: *m/z* 547.3272 [M+H]⁺ (calcd for C₃₁H₄₇O₈: 547.3265); *t_R* = 14.4 min.

Fragarubrin G (**6**): yellow oil; $[\alpha]_D = -2$ (*c* = 0.1, MeCN); ¹H NMR (CDCl₃, 700 MHz): see Table 1; ¹³C NMR (CDCl₃, 175 MHz): see Table 2; IR (ATR): $\tilde{\nu}_{\max} = 2924, 2854, 1737, 1717, 1641, 1233$ cm⁻¹, see Figure S42; UV/Vis (MeCN): $\lambda_{\max} (\epsilon) = 218$ (4.23), 327 (4.20) nm; ECD (MeCN) $\lambda(\Delta\epsilon) = 199$ (−5.3), 232 (+1.4), 249 (−0.9), 272 (+3.8), 321 (−3.8) nm, see Figure S44 in the Supporting Information; ESI-MS: *m/z* 529.38 [M+H]⁺, 527.24 [M−H][−]; HR-ESI-MS: *m/z* 529.3160 [M+H]⁺ (calcd for C₃₁H₄₅O₇: 529.3160); *t_R* = 17.5 min.

Mosher's analyses

For the preparation of the (*S*)-MTPA ester 1 mg of hybridorubrin A (**1**) was dissolved in 600 μL of $[\text{D}_5]$ pyridine, and 10 μL of (*R*)-MTPA chloride was added. The mixture was incubated at 25 °C for 15 min and ^1H NMR, $^1\text{H}/^1\text{H}$ COSY, $^1\text{H}/^{13}\text{C}$ -HSQC, and $^1\text{H}/^{13}\text{C}$ -HMBC spectra were measured. ^1H NMR (700 MHz, $[\text{D}_5]$ pyridine): similar to **1**, but $\delta_{\text{H}} = 1.22$ (11'- H_2), 1.60 (12'- H_2), 5.29 (13'-H), 1.63 (14'- H_2), 1.37 (15'- H_2), 0.88 ppm (16'- H_3). The (*R*)-MTPA ester was prepared in the same manner by addition of 10 μL of (*S*)-MTPA chloride: ^1H NMR (700 MHz, $[\text{D}_5]$ pyridine): similar to that of **1**, but $\delta_{\text{H}} = 1.67$ (12'- H_2), 5.30 (13'-H), 1.57 (14'- H_2), 1.23 (15'- H_2), 0.82 ppm (16'- H_3). Results are depicted in Figure S38 in the Supporting Information.

Hybridorubrin B (2×0.7 mg, **2**) was converted analogously. (*S*)-MTPA ester of **2**: ^1H NMR (700 MHz, $[\text{D}_5]$ pyridine): similar to **2**, but $\delta_{\text{H}} = 2.09$ (14'- H_2), 1.69 (15'- H_2), 5.23 (16'-H), 1.68 (17'- H_2), 0.91 ppm (18'- H_3). (*R*)-MTPA ester of **2**: ^1H NMR (700 MHz, $[\text{D}_5]$ pyridine): similar to that of **2**, but $\delta_{\text{H}} = 2.24$ (14'- H_2), 1.75 (15'- H_2), 5.24 (16'-H), 1.62 (17'- H_2), 0.80 ppm (18'- H_3). Results are depicted in Figure S39 in the Supporting Information.

Hybridorubrin C (2×0.5 mg, **3**) was converted analogously. (*S*)-MTPA ester of **3**: ^1H NMR (700 MHz, $[\text{D}_5]$ pyridine): similar to **3**, but $\delta_{\text{H}} = 1.20$ (15'- H_2), 1.59/1.47 (16'- H_2), 5.27 (17'-H), 1.30 ppm (18'- H_3). (*R*)-MTPA ester of **3**: ^1H NMR (700 MHz, $[\text{D}_5]$ pyridine): similar to **3**, but $\delta_{\text{H}} = 1.33$ (15'- H_2), 1.67/1.52 (16'-H), 5.26 (17'- H_2), 1.24 ppm (18'- H_3). Results are depicted in Figure S40 in the Supporting Information.

Fragirubrin F (2×0.5 mg, **5**) was converted analogously. (*S*)-MTPA ester of **5**: ^1H NMR (700 MHz, $[\text{D}_5]$ pyridine): similar to **5**, but $\delta_{\text{H}} = 1.21$ (12'- H_2), 1.69/1.57 (13'- H_2), 5.18 (14'-H), 1.66 (15'- H_2), 0.92 (16'- H_3) ppm. (*R*)-MTPA ester of **5**: ^1H NMR (700 MHz, $[\text{D}_5]$ pyridine): similar to **5**, but $\delta_{\text{H}} = 1.36$ (12'- H_2), 1.61/1.54 (13'- H_2), 5.19 (14'-H), 1.36 (15'- H_2), 0.81 (16'- H_3) ppm. Results are depicted in Figure S41 in the Supporting Information.

Epoxidation and MS/MS measurements of 3

To locate the position of the double bond in the fatty acid moiety of hybridorubrin C (**3**), a sample was epoxidized with *meta*-chloroperoxybenzoic acid (mCPBA) followed by MS/MS analysis, as recently published:^[14] at first, 10 μg of **3** was incubated with 10 μg of mCPBA in 10 μL of CH_2Cl_2 at room temperature. The reaction was quenched after 10 min with 490 μL of CH_2Cl_2 :MeCN (1:1). The same procedure was applied to an authentic reference sample of *cis*-octadecenoic acid [C18:1(9)].

Then, 1 μL of the samples was injected into an UltiMate 3000 Series uHPLC (Thermo Fisher Scientific) equipped with a C18 Kinetex column (1.7 μm , 150 \times 2.1 mm, Phenomenex, Torrance, CA/USA) and the following gradient of H_2O +0.1% formic acid (A) and MeCN+0.1% formic acid (B): 1% B for 2 min, increasing to 100% B over 18 min, keeping 100% B for further 4 min, flow rate 0.3 mL min⁻¹. This HPLC was connected to a maxis HD UHR-ESI-QTOF-MS (Bruker) with the following parameters: scan range: m/z 50–1500, ion polarity: negative, capillary voltage: 4500 V, nebulizer pressure: 4.0 bar, dry heater: 200 °C, dry gas: 9.0 L min⁻¹, collision energy: 20.3–50.7 eV. Results are depicted in Figure S45.

GC analysis of 6

To determine the double-bond geometry of the palmitoleic acid moiety of fragirubrin G (**6**), 0.5 mg of the compound was hydrolysed by incubating it with MeOH/NaOH (15%) 1:1 for 1 h at 100 °C to yield **6**-fatty acid (**6**-FA). Then, **6**-FA, as well as of 9-*cis*- and 9-

trans-hexadecenoic acid references, were derivatised to yield fatty acid methyl esters (FAMES) by incubating them in MeOH/HCl (37% w/v) 5:1 for 10 min at 80 °C. Afterwards, the three samples were extracted into the organic phase as described previously.^[34] The samples were analysed by gas chromatography with an Agilent 6890N GC with flame ionization detector. Separation of the FAMES was carried out with a Macherey-Nagel Optima 5 column (5% phenyl, 95% dimethylpolysiloxane; 50 m length; 0.32 mm inner diameter; 0.25 μm film thickness). The retention time of **6**-FAME was compared with those of both references to identify its double-bond configuration. The result is depicted in Figure S46 in the Supporting Information.

Bioassays

Minimum inhibitory concentrations (MICs) were determined as described previously.^[35] A detailed protocol is given in the Supporting Information. Various test organisms of fungal and bacterial origin were tested. Bacteria: *Bacillus subtilis* (DSM10), *Staphylococcus aureus* (DSM346), *Micrococcus luteus* (DSM1790), *Chromobacterium violaceum* (DSM30191), *Escherichia coli* (DSM1116), *Pseudomonas aeruginosa* (PA14); Mycobacteria: *Mycobacterium smegmatis* (ATCC700084); Fungi: *Candida albicans* (DSM1665), *Schizosaccharomyces pombe* (DSM70572), *Mucor hiemalis* (DSM2656), *Pichia anomala* (DSM6766), *Rhodotorula glutinis* (DSM10134). Results are listed in Table S3 in the Supporting Information.

The cytotoxicity assay against mouse fibroblast cell line L929 and human cervical cancer cell line KB 3.1 was performed as described before.^[36] Results are depicted in Table S3 in the Supporting Information.

The biofilm formation inhibition assay against *Staphylococcus aureus* (DSM1104) was conducted as described before.^[37] Results are listed in Table 3.

Bioinformatic analysis for gene cluster prediction

The genome of the *H. fragiforme* strain MUCL 51264 was sequenced by using PacBio, and gene prediction and annotation were carried out as previously described.^[10] Candidate gene clusters were manually identified by blast searches by using various protein sequences as templates (UniProtKB/Swiss-Prot: G3XMC4, G3XMC1, G3XMB9) against a created *H. fragiforme* protein database. The searches were performed with the software Geneious 9.1.8 (<https://www.geneious.com>). Homology between related biosynthetic gene cluster was mapped and visualized with the clinker tool.^[38] The identified gene cluster were uploaded to GenBank under the accession numbers MN736720 (*hfaza2*) and MN736721 (*hfaza1*).

Acknowledgements

The authors wish to thank Silke Reinecke and Anke Skiba for expert assistance in the lab. We are also grateful for the help of Aileen Gollasch and Klaus-Peter Conrad for recording the HR-ESI-MS spectra, as well as Christel Kakoschke for performing the NMR measurements. Furthermore, Ulrike Beutling is thanked for assistance with MS/MS measurements. We would like to thank Lucile Wendt for providing the stromatal material and the photograph for the table of contents graphic. In addition, we would like to thank Hedda Schrey and Tian Cheng for support with the bioassays as well as Lulu Shao for assistance

with the isolation procedure. Boyke Bunk and Cathrin Spröer are acknowledged for PacBio sequencing and Daniel Wibberg for genome annotation. Sebastian Riesinger, Kimberly Borkiet and Natascha Stomberg are thanked for their work in their practical laboratory courses. K.B., E.K., R.J.C., and M.S. are grateful for a grant from the Deutsche Forschungsgemeinschaft (DFG CO 1328/4-1) in the Priority Programme "Taxonomics: New Approaches for Discovering and Naming Biodiversity" (SPP 1991). Open access funding enabled and organized by Projekt DEAL.

Conflict of interest

The authors declare no conflict of interest.

Keywords: biosynthesis · inhibitors · natural products · polyketides · structure elucidation

- [1] a) L. Wendt, E. B. Sir, E. Kuhnert, S. Heitkämper, C. Lambert, A. I. Hladki, A. I. Romero, J. J. Luangsa-ard, P. Srikitikulchai, D. Peršoh, M. Stadler, *Mycol. Prog.* **2018**, *17*, 115–154; b) F. Surup, A. Narmani, L. Wendt, S. Pfütze, R. Kretz, K. Becker, C. Menbrivès, A. Giosa, M. Elliott, C. Petit, M. Rohde, M. Stadler, *Fungal Divers.* **2018**, *92*, 345–356.
- [2] S. E. Helaly, B. Thongbai, M. Stadler, *Nat. Prod. Rep.* **2018**, *35*, 992–1014.
- [3] W. Steglich, M. Klaar, W. Furtner, *Phytochemistry* **1974**, *13*, 2874–2875.
- [4] M. Stadler, D. N. Quang, A. Tomita, T. Hashimoto, Y. Asakawa, *Mycol. Res.* **2006**, *110*, 811–820.
- [5] J. R. Anderson, R. L. Edwards, A. J. S. Whalley, *J. Chem. Soc. Perkin Trans. 1* **1983**, 2185–2192.
- [6] R. L. Edwards, V. Fawcett, D. J. Maitland, R. Nettleton, L. Shields, A. J. S. Whalley, *J. Chem. Soc. Chem. Commun.* **1991**, 1009–1010.
- [7] a) R. Kretz, L. Wendt, S. Wongkanoun, J. J. Luangsa-Ard, F. Surup, S. E. Helaly, S. R. Noumeur, M. Stadler, T. E. B. Stradal, *Biomolecules* **2019**, *9*, 73; b) J. Ondeyka, O. D. Hensens, D. Zink, R. Ball, R. B. Lingham, G. Bills, A. Dombrowski, M. Goetz, *J. Antibiot.* **1992**, *45*, 679–685.
- [8] K. T. Yuyama, C. Chepkirui, L. Wendt, D. Fortkamp, M. Stadler, W. R. Abraham, *Microorganisms* **2017**, *5*, 80.
- [9] D. Wibberg, M. Stadler, C. Lambert, B. Bunk, C. Spröer, C. Rückert, J. Kalinowski, R. J. Cox, E. Kuhnert, *Fungal Divers.* **2020**, <https://doi.org/10.1007/s13225-020-00447-5>.
- [10] C. Wang, K. Becker, S. Pfütze, E. Kuhnert, M. Stadler, R. J. Cox, E. Skellam, *Org. Lett.* **2019**, *21*, 8756–8760.
- [11] T. R. Hoye, C. S. Jeffrey, F. Shao, *Nat. Protoc.* **2007**, *2*, 2451–2458.
- [12] E. Kuhnert, F. Surup, E. B. Sir, C. Lambert, K. D. Hyde, A. I. Hladki, A. I. Romero, M. Stadler, *Fungal Divers.* **2015**, *71*, 165–184.
- [13] E. Alexandri, R. Ahmed, H. Siddiqui, M. I. Choudhary, C. G. Tsiafoulis, I. P. Gerathanassis, *Molecules* **2017**, *22*, 1663.
- [14] Y. Feng, B. Chen, Q. Yu, L. Li, *Anal. Chem.* **2019**, *91*, 1791–1795.
- [15] F. D. Gunstone, M. R. Pollard, C. M. Scrimgeour, H. S. Vedanayagam, *Chem. Phys. Lipids* **1977**, *18*, 115–129.
- [16] G. Büchi, J. D. White, G. N. Wogan, *J. Am. Chem. Soc.* **1965**, *87*, 3484–3489.
- [17] S. Suzuki, T. Hosoe, K. Nozawa, T. Yaguchi, S. Udagawa, K. Kawai, *J. Nat. Prod.* **1999**, *62*, 1328–1329.
- [18] R. C. Clark, S. Y. Lee, D. L. Boger, *J. Am. Chem. Soc.* **2008**, *130*, 12355–12369.
- [19] C. Chepkirui, K. T. Yuyama, L. A. Wanga, C. Decock, J. C. Matasyoh, W. R. Abraham, M. Stadler, *J. Nat. Prod.* **2018**, *81*, 778–784.
- [20] a) A. al Fahad, A. Abood, T. J. Simpson, R. J. Cox, *Angew. Chem. Int. Ed.* **2014**, *53*, 7519–7523; *Angew. Chem.* **2014**, *126*, 7649–7653; b) W. Chen, R. Chen, Q. Liu, Y. He, K. He, X. Ding, L. Kang, X. Guo, N. Xie, Y. Zhou, Y. Lu, R. J. Cox, I. Molnar, M. Li, Y. Shao, F. Chen, *Chem. Sci.* **2017**, *8*, 4917–4925; c) Y. He, R. J. Cox, *Chem. Sci.* **2016**, *7*, 2119–2127.
- [21] A. O. Zabala, W. Xu, Y. H. Chooi, Y. Tang, *Chem. Biol.* **2012**, *19*, 1049–1059.
- [22] P. C. Woo, C. W. Lam, E. W. Tam, C. K. Leung, S. S. Wong, S. K. Lau, K. Y. Yuen, *PLoS Neglected Trop. Dis.* **2012**, *6*, e1871.
- [23] a) A. Abood, A. Al-Fahad, A. Scott, A. E.-D. M. S. Hosny, A. M. Hashem, A. M. A. Fattah, P. R. Race, T. J. Simpson, R. J. Cox, *RSC Adv.* **2015**, *5*, 49987–49995; b) A. R. Benitez, S. Tweedy, S. A. Baker Dockrey, A. L. Lukowski, T. Wymore, D. Khare, C. L. Brooks 3rd, B. A. Palfey, J. L. Smith, A. R. H. Narayan, *ACS Catal.* **2019**, *9*, 3633–3640.
- [24] B. Bonsch, V. Belt, C. Bartel, N. Duensing, M. Koziol, C. M. Lazarus, A. M. Bailey, T. J. Simpson, R. J. Cox, *Chem. Commun.* **2016**, *52*, 6777–6780.
- [25] note: no stereochemistry was reported for the respective compounds, thus it might differ from **8** and **10** reported herein.
- [26] X. Xie, K. Watanabe, W. A. Wojcicki, C. C. Wang, Y. Tang, *Chem. Biol.* **2006**, *13*, 1161–1169.
- [27] K. M. Fisch, E. Skellam, D. Ivison, R. J. Cox, A. M. Bailey, C. M. Lazarus, T. J. Simpson, *Chem. Commun.* **2010**, *46*, 5331–5333.
- [28] D. N. Quang, T. Hashimoto, M. Stadler, Y. Asakawa, *Tetrahedron* **2005**, *61*, 8451–8455.
- [29] Y. Tabata, S. Ikegami, T. Yaguchi, T. Sasaki, S. Hoshiko, S. Sakuma, K. Shin-Ya, H. Seto, *J. Antibiot.* **1999**, *52*, 412–414.
- [30] H. Ming Ge, W. Yun Zhang, G. Ding, P. Saparpakorn, Y. Chun Song, S. Hannongbua, R. X. Tan, *Chem. Commun.* **2008**, 5978–5980.
- [31] X. Huang, W. Zhang, S. Tang, S. Wei, X. Lu, *Angew. Chem. Int. Ed.* **2020**, *59*, 4349–4353; *Angew. Chem.* **2020**, *132*, 4379–4383.
- [32] V. Hantke, C. Wang, E. J. Skellam, R. J. Cox, *RSC Adv.* **2019**, *9*, 35797–35802.
- [33] a) E. Kuhnert, F. Surup, V. Wiebach, S. Bernecker, M. Stadler, *Phytochemistry* **2015**, *117*, 116–122; b) D. N. Quang, T. Hashimoto, M. Stadler, Y. Asakawa, *J. Nat. Prod.* **2004**, *67*, 1152–1155.
- [34] W.-R. Abraham, C. Hesse, *FEMS Microbiol. Ecol.* **2003**, *46*, 121–128.
- [35] F. Surup, S. Halecker, M. Nimtz, S. Rodrigo, B. Schulz, M. Steinert, M. Stadler, *Steroids* **2018**, *135*, 92–97.
- [36] K. Becker, A.-C. Wessel, J. J. Luangsa-Ard, M. Stadler, *Biomolecules* **2020**, *10*, 805.
- [37] K. T. Yuyama, L. Wendt, F. Surup, R. Kretz, C. Chepkirui, K. Wittstein, C. Boonlarppradab, S. Wongkanoun, J. J. Luangsa-ard, M. Stadler, W. R. Abraham, *Biomolecules* **2018**, *8*, 129.
- [38] C. L. M. Gilchrist, Y.-H. Chooi, *bioRxiv* **2020**, doi: 10.1101/2020.11.08.370650.

Manuscript received: July 7, 2020

Accepted manuscript online: August 4, 2020

Version of record online: December 10, 2020